ORIGINAL ARTICLE

lajss.org Latin American Journal of Solids and Structures www.lajss.org

Reducing the cost of calculations for stability analysis of tall buildings using a new approach

Javad Firouzbakhsh[a], Mohsen Malekinejad[b], Reza Rahgozar[c]*

[a]Department of Civil Engineering, Shahid Bahonar University of Kerman, Kerman, Iran. Email: javad_firoozbakhsh@eng.uk.ac.ir
[b]Department of Civil Engineering, Sirjan Branch, Islamic Azad University, Sirjan, Iran. Email: malekinejad.mohsen@iau.ac.ir
[c]Department of Civil Engineering, Shahid Bahonar University of Kerman, Kerman, Iran. Email: rahgozar@uk.ac.ir

*Corresponding author

https://doi.org/10.1590/1679-78258003

Abstract
This research proposes an innovative method to convert the modeling of three-dimensional structures to the modeling of two-dimensional structures for the stability analysis of long tubular buildings. The process of the proposed method is in the form of modeling the equivalent frame and then modeling the reduced frame using the equivalent moment of inertia for beams and columns. The second-order elastic analysis has been performed considering the effects of P-Δ and P-δ. Framed-tube and frame tube-in-tube systems have been used for modeling. Newton's Raphson and Crisfield's Arc Length methods have also been used for nonlinear analysis. The accuracy and speed of analysis of the new method have been checked by comparing the displacements and drifts in the modeled systems for 40 and 50 stories tall buildings. For each structure, two framed-tube and tube-in-tube systems are considered. In the presented method, the number of nodes and elements in the reduced model is much less. The method presented in this research can reduce the amount of calculating the response of tall structures and the duration of the analysis. One of the advantages of the presented method is the acceptable accuracy of the analysis along with the high speed of the analysis. The results show that the proposed method has reduced the amount of calculations by 80% along with a 5% reduction in the accuracy of structural responses.

Keywords
Tall buildings, Framed-tube, Framed tube-in-tube, Stability analysis.

Graphical Abstract

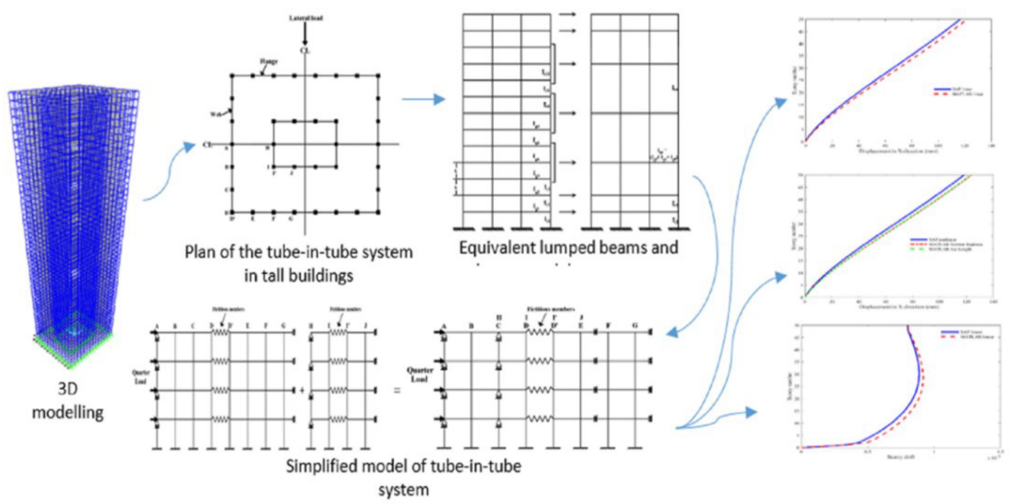

Received: January 23, 2024. In revised form: June 04, 2024. Accepted: July 01, 2024. Available online: July. 02, 2024.
https://doi.org/10.1590/1679-78258003

1 INTRODUCTION

In recent decades, framed tube structures with different heights have been built as an economic system in international communities (Ali and Al-Kodmany, 2022). The framed tube consists of closely spaced columns connected by relatively deep spandrels (Taranath, 2016). Framed tube systems are divided into three categories: a) systems without internal columns, shear walls, or steel braces; b) systems with internal columns, shear walls, or steel braces and c) tube-in-tube systems. By using the framed tube system, it is possible to resist lateral oscillation loads up to a height of more than 100 stories (Gunel and Ilgin, 2007; Hosseini et al., 2012). Researchers have proposed many approximate analysis methods as an alternative to the finite element method to simplify the calculations in the initial design of framed tubes. Horizontal vibration analysis is generally done using approximate analysis. In the approximate method using the transfer matrix, the dynamic response of the structure such as displacement, rotation, bending moment, and shear forces are described as a transfer vector (Li et al., 2010; Rahgozar et al., 2010; Bozdogan and Ozturk, 2014; Lavanya and Sridhar, 2017). To simplify the analysis, researchers have proposed different methods for modeling and analysis. Rahgozar et al. using a mathematical model obtained the best position of the belt truss in building height with a combined system of frame-tube, shear core, and belt truss system (Rahgozar and Sharifi, 2009). Takabatake (2010) formulated the governing equation for two-dimensional bar theory by imposing continuity conditions across the boundary between distinct structural components in the transverse direction. A mathematical model has been used by Dadkhah et al. (2022) and Rahgozar (2020) to calculate the natural frequencies and corresponding mode shapes of a tall building with a belt truss system. A parametric function has been presented by Jahanshahi et al. (2012) for static analysis of tall buildings with combined tube-in-tube and outrigger-belt truss systems by considering shear lag effects based on the principle of minimum total potential energy. The structure has been modeled by two continuous cantilever beams which are restrained at the outrigger-belt truss location by a rotational spring. The proposed formulas yield reasonable results obtained from three-dimensional studies using the finite element method.

Several researchers have been studied stability analysis of tall buildings (Hariri-Ardebili et al., 2014). Zalka (1979) studied buckling analysis of a cantilever subjected to distributed normal loads considering shear deformation and an approximate solution has been used to develop a curve for critical load. In another study carried out by Zalka (2002), a simple analytical hand calculation method is presented for the three-dimensional stability analysis of buildings braced by frameworks, coupled shear walls, shear walls and cores. Sway buckling behaviour has been considered by three types of deformation. Based on the stiffnesses associated with these three types of deformation, a closed formula has been derived for the calculation of the sway critical load. A 73 multistorey buildings with step by step instructions shows the easy use of the method. Parv and Nicoreac (2012) used the approximate method based on the equivalent column theory for structural stability analysis of tall reinforced concrete buildings. A method is proposed for designating the critical buckling load of system consists of frames and shear walls by Aydin and Bozdogan (2016). In this study, the multistory uniform structure is modeled in accordance with the continuous system calculation model and the differential equation governing the stability case is solved using the differential transform method. The examples solved shows that the results obtained from the differential transform method are in sufficient conformity with the results obtained from the finite elements method. The differential transform method provides easy and fast solutions. Also it has been concluded that the presented method can be relied upon to both easily understand the behavior of the structure and check the results obtained using the finite elements method. In 2024, researchers experimentally obtained the cyclic performance of a new tube-in-tube buckling brace (BRB) configuration. They showed that tube-in-tube BRBs are able to develop stable compressive and tensile stress hysteretic behavior during cyclic loading (Prinz and Richards, 2024). One of the seismic-resistant systems widely used worldwide is the tube-in-tube system. In the review paper, the scientists presented a comprehensive exploration of seismic analysis methods with a special focus on their application in tube-in-tube structures characterized by constant cross-sectional area according to Sharma and Gurjar (2024).

Numerous studies have been focusing on how a 3D model can be transformed into a convenient 2D model, such as FEMA P695. Tehranizadeh et al. tried to clarify a new simple approach to conform a 3D symmetric reinforced concrete core wall system. It can be applied to any symmetric and regular reinforced concrete core wall systems, regardless of their wall size and thickness, and building height (Tehranizadeh et al., 2019). A comparative analysis between tube-in-tube structure and conventional moment-resisting system has been carried out by Naik and Chandra (2017). The main objective of their study was to compare the tube in tube structure with moment resisting frame. Framed tube structures with various internal tubes which are also termed as tubes in tube structure, have high strength for resisting horizontal load and the inner tubes are vertical tubes. These structures when come in contact with a parallel load like wind load, the corner sections experience higher axial load because of shear lag. Tall buildings against natural hazards which created by wind and earthquakes are usually associated with the analysis of structural stability according to Dua and Jain (2004); Li et al. (2021) and Li et al. (2022).

In this article, a simplified method for analyzing the stability of a structure with tube-in-tube systems has been done. First, the real structure was modeled in 2D form, then the 2D structure was converted into a reduced two-dimensional structure, then the corresponding results were obtained. Using finite element matrix analysis, linear analysis was performed, and then geometric nonlinear analysis was also performed using Arc Length and Newton's Raphson methods. The critical buckling load has also been calculated using linear and geometric matrices. Finally, the drift of the structure has been obtained and the stability of the structure has also been investigated.

2 PROCEDURES

2.1 Analysis

The actual behavior of structures is nonlinear and complex. Different levels of analysis can be used to analyze and design structures. In recent decades, more complex techniques can be used for analysis due to the availability of powerful computers. Fig. 1 shows the generalized load versus deflection path for general analysis types for framed structures. In linear analysis, the applied force is assumed to be proportional to the deflection. Tracing the path of equilibrium or load against the deflection path is one of the precise methods of structural analysis. Considering the effects of *P-δ* and *P-Δ*, the effects of primary defects can be included in a detailed analysis. These effects are important for slender structures. In the second-order elastic analysis, the effects of the second-order analysis due to the change of geometry and initial stress in the members are considered Chan and Chui (2000).

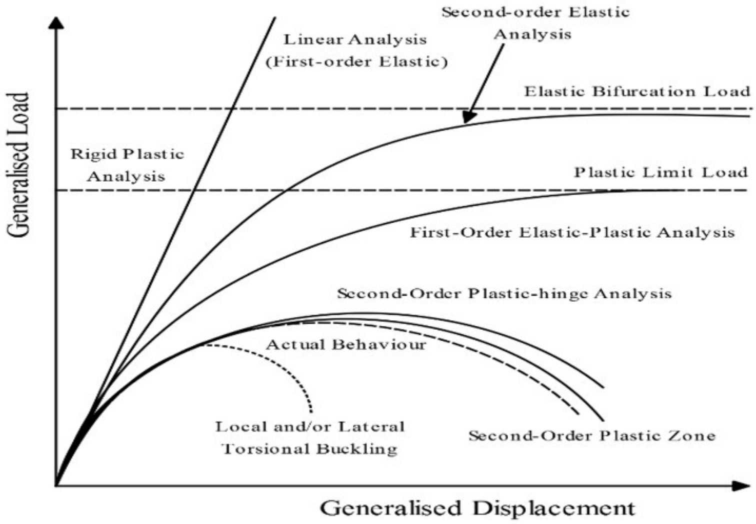

Figure 1 General analysis types for framed structures (Chan and Chui, 2000).

2.2 Formulation

For small deformations the stiffness does not change during the application of load, but in the case of large deformations the stiffness changes during the load application. So, the loads are applied gradually at different stages and the stiffness is updated at different stages of loading. Buckling occurs when the stiffness of the structure tends to zero during the application of compressive forces. Buckling can cause the structure to collapse. If it passes through the buckling stage, it can cause new stiffness. The force that caused buckling can be obtained using linear buckling analysis. Also, the idealization of structures in finite element analysis may cause the predicted results for buckling load to be much higher than the actual value. Therefore, caution should be used in using linear buckling analysis. By using nonlinear analysis, the behavior after buckling can be described. In this research, a nonlinear analysis focusing on geometric nonlinearity and investigating the stability of the building with a nested environmental frame system has been done. In relation, I, the total moment of inertia is the sum of two interior and exterior moments of inertia. The properties and variables related to the exterior framed tube are displayed with index e and for the interior framed tube with index i:

$$EI = (EI)_i + (EI)_e \tag{1}$$

Where EI is the sum of the bending stiffness of the interior and exterior framed tubes, E is the modulus of bending elasticity, A is the cross-section of the columns and I is the moment of inertia of the interior and exterior framed tubes.

2.3 Geometric nonlinear analysis

As shown in Fig. 2, the prismatic element of two symmetrical sections is subjected to an axial force and bent around the z-axis. Shear deformation is omitted. This element loading provides a formulation of stiffness properties for geometric nonlinear analysis. Displacement can be considered as a function of rigid body end rotation, shortening, stretching, or bending. All things can happen at the same time and affect each other. However, to focus on the most important effects, the total displacement can be considered as the stretching and rotation of the rigid body or the bending of the element relative to the chord. For this purpose, two geometric stiffness matrices have been created. The first is for the case where there is no bending and the problem is reduced to a straight member subjected to rotation and axial strain of Fig. 3. The second one is for a member subjected to a combined axial and bending force McGuire et al. (2000).

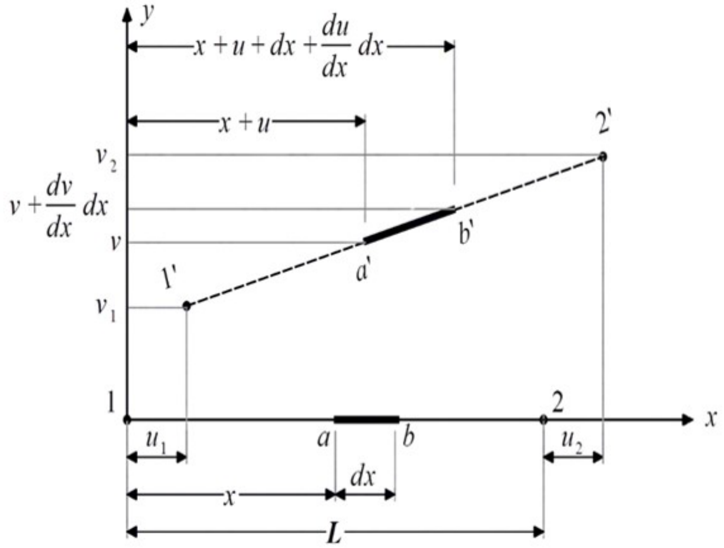

Figure 2 Stretching and rigid body rotation of axis (McGuire et al., 2000).

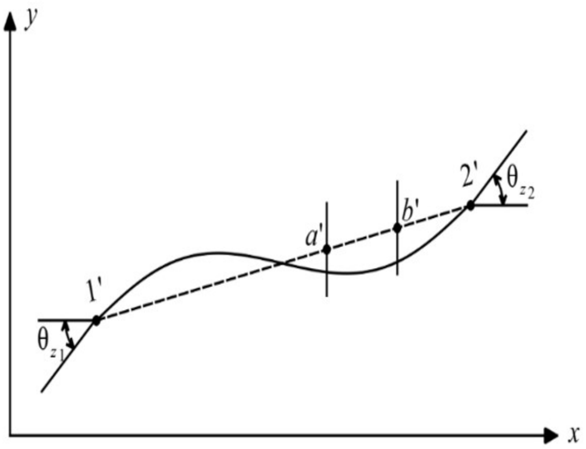

Figure 3 Flexure of the element with respect to the chord joining the displaced ends (McGuire et al., 2000)

For the tube-in-tube system, the elastic stiffness matrix [K_e] is obtained as the sum of the stiffness matrix of the interior framed tube, [Kei], and the exterior framed tube, [K_{ee}]:

$$[K_e] = [K_{ei}] + [K_{ee}] \tag{2}$$

In addition, for the tube-in-tube systems, the geometric stiffness matrix for the geometric nonlinear analysis [K_g] obtained by the sum of the geometric stiffness matrix of the interior framed tube, [K_{gi}], and the exterior framed tube, [Kge]:

$$\left[K_g\right] = \left[K_{gi}\right] + \left[K_{ge}\right] \tag{3}$$

Therefore, the total stiffness matrix for the geometric nonlinear analysis of the tube-in-tube systems, [K_T], is written as follows using the sum of Eqs. (2) and (3):

$$\left[K_T\right]=\left[K_e\right]+\left[K_g\right] \tag{4}$$

2.4 Proposed method

In this section, an approximate mathematical model for calculating the linear and geometric stiffness matrix of tall buildings with a tube-in-tube system is presented. Because the plan of the structure is symmetrical in two directions, a quarter of the external framed tube (ABCDEFG(and a quarter of the internal frame tube)HIJ(as shown in Fig.4 have been considered for analysis. The load applied to the equivalent flat frame is equal to a quarter of the load on the main structure. Instead of connecting the interior framed tube to the exterior framed tube, we used another method and placed the interior framed tube in the middle of the exterior framed tube. Therefore, the coding process becomes easier. The internal and external frames are symmetrical in the tube-in-tube systems, with the same assumption of the stiffness matrix of the external frame that was formed, another stiffness matrix with the same number of rows and columns of the stiffness matrix of the external frame with zero degrees was also made for the internal frame. When assembling the stiffness matrix, the internal frame tube reservoirs are formed and it is also possible to sum up with the stiffness matrix of the external frame tube. Then we apply the boundary conditions at the intersection of the internal and external frames and the support conditions and analyze the equivalent flat two-dimensional frame. The methods used in this article for tube-in-tube systems analysis are linear analysis and geometric nonlinear analysis, and Newton's Raphson and Arch Length methods are also used to solve nonlinear equations. The Newton's Raphson method is described in Appendix A. The Arch Length method is described in Appendix B. In addition, the critical load of buckling is obtained by eigenvalue values and eigenvalue vectors, and finally the drift of the structure is also calculated to check the stability.

Also, the following assumptions prevail in this research:

a. The behavior of materials is considered linear elastic and follows Hooke's law.

b. Floor slabs are rigid in their plane.

c. The characteristics of the structure as well as the space between the columns along the height are to be uniform.

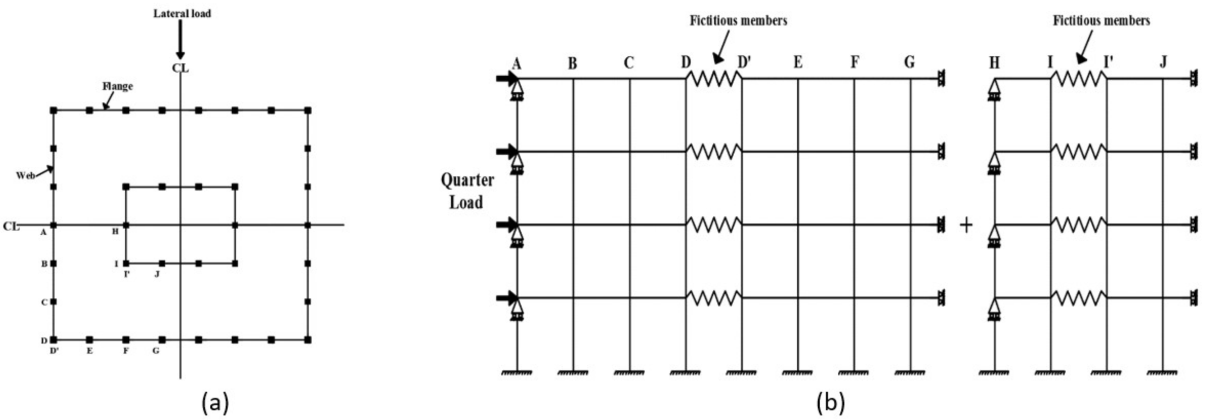

Figure 4 Tube-in-tube system in tall buildings; (a) Quarter model of tube-in-tube system, (b) Simplified model of tube-in-tube system

2.5 Simplification of rigid frames with equivalent beams

In buildings with repeated stories, it is possible to combine several beams together and create a model with fewer stories. From the analysis of the frame with concentric beams, accurate results for the displacement and a good estimate of the member forces are obtained. The beams of the first story and the roof should not be included in the concentrated sets, because the behavior of the frame at the top and bottom is very different from its middle range. The working method is exactly the same as the method mentioned in the modeling part of the equivalent flat frame, with the difference that the amount of load that was applied to the equivalent frame as a quarter of the original load is also applied to the reduced model as n times the applied load. Where, n equal to the reduction factor. For example, to convert a 13-story building into a reduced 7-story model, n is equal to 3 (see Fig. 5)) Smith and Coull (1991).

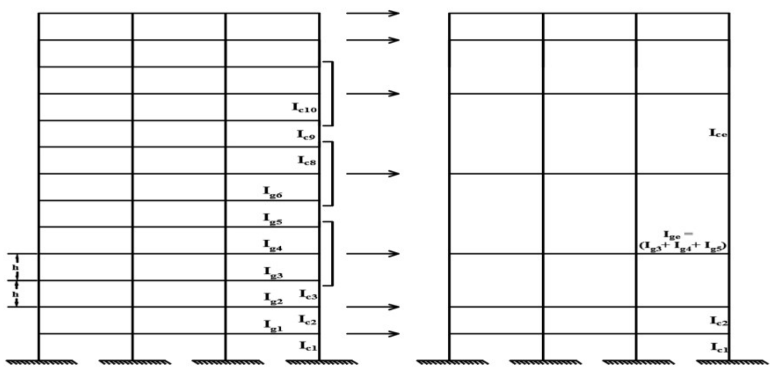

(a) (b)

Figure 5 (a) Rigid frame with repetitive beams; (b) Equivalent lumped beam model (Smith and Coull, 1991)

In a simplified frame, the displacement of the horizontal load should be equal to the displacement of the primary structure (Kwan, 1994; Davari et al., 2019). The condition of equality of change of transitional places of the primary structure with the change of transitional places caused by bending of the beams, through the following relationship (Malekinejad and Rahgozar, 2011; Malekinejad and Rahgozar, 2012; Rahgozar et al., 2015):

$$\delta_{ig} = \frac{Q_i h^2{}_i}{12E\sum\left(\frac{I_g}{L}\right)_i} \tag{5}$$

By replacing the total inertias of n groups of main beams instead of the inertia of the equivalent beam is satisfied:

$$I_{ge} = \sum_{i=1}^{n} I_g \tag{6}$$

To determine the properties of columns in the equivalent frame, displacement caused by bending of two curvatures of the column at a height of (nh) in the equivalent frame is equal to the corresponding displacement of n stories of the main frame:

$$\frac{Q(nh)^2}{12E\sum I_{ce}/nh} = \frac{Qh^2}{12E}\sum_{i=1}^{n}\frac{1}{\sum\left(I_c/h\right)_i} \tag{7}$$

In the above relation, the moment of inertia of the equivalent column is:

$$I_{ce} = \frac{n^3}{\sum_{i=1}^{n}\left(\frac{1}{I_c}\right)_i} \tag{8}$$

Where, I_g, I_c, I_{ge}, I_{ce}, E, Q_i, h, δ_{ig}, n, and L are the moment of inertia of girders, the moment of inertia of columns, the equivalent moment of inertia of girders, the equivalent moment of inertia of columns, Young's modulus, external shear force, story height, displacement of story ith, the number of stories in equivalent frames and bay width, respectively.

For linear analysis, we use the equation mentioned above for the stiffness matrix in linear mode, and displacements and rotations will be obtained. For nonlinear and buckling analysis, we will act according to the equations mentioned for the stiffness matrix, so there are several numerical methods for solving with their advantages and disadvantages. There are many methods to analyze nonlinear problems. The most important of these methods are the load control method, displacement control method, arc length method, and work control method. Such methods are also called prediction-correction methods because they predict the answer in one increment and correct the answer with a series of repetitions. The load control method is one of the oldest nonlinear analysis methods. In this article, Newton's Raphson increment-iterative method and arc length method are used, which reduces the cumulative error to the minimum possible by performing several repetitions in each development. In the analysis of tall structures, due to the increase of floors and as a result of the increase in the degrees of freedom of the structure, it has been tried to find a solution to reduce the dimensions of the matrices to save time and increase the speed of operation by using the proposed methods. Similar floors and reducing the number of beams and columns and finally using equivalent beams and columns became possible. Using one of the important topics of stability, i.e., the secondary effects of vertical loads on the lateral displacement caused by horizontal loads, or the primary defect of the structure in the vertical direction, which is the same as the effects first one, and also by using non-linear analysis methods, codes were written in the MATLAB program environment (MATLAB, R2018a). It has been compared with SAP2000 software (SAP2000, Version 22.2.0), which controls the stability of the structure with very high accuracy, and favorable results have also been presented.

3 NUMERICAL EXAMPLES

For numerical examples and verification, a 40-story structure with a frame tube system was done in 3D in SAP2000 software and verified with the values in the article. Then, the relevant example was converted into a structure with a tube-in-tube system, and relevant analyses were performed in MATLAB software. In addition, a 50-story example with two systems of frame tube and tube-in-tube was also investigated. The results and related graphs are also given at the end.

3.1 Example 1:

In this example, two high-rise 40-story concrete models have been used. The first is the framed-tube structure with the reduced model and the second is the tube-in-tube structure with the reduced model Kwan (1994). The dimensions of beams and columns are 0.8 meters by 0.8 meters. Floors are modeled with a height of 3.0 meters and columns with a distance of 2.5 meters. The modulus of elasticity is considered to be 20 GPa. Lateral load and vertical load are applied with a uniform distribution of 120 kN/m and 200 kN/m, respectively on the structures. Specifications of the structure are listed in Tables 1 and 2. Plan layout, elevation view, and 3D modeling of this example have been shown in Fig. 6. Also, displacements and rotations of the tubular structure are shown in Tables 3-5 and Figs. 7-15.

Table 1 Dimensions of 40-story buildings

External frame tube dimensions		Internal frame tube dimensions		Distance from center to center of the columns		Story height
$2(W_f)_o$ (m)	$2(W_w)_o$ (m)	$2(W_f)_i$ (m)	$2(W_w)_i$ (m)	S_f (m)	S_w (m)	h (m)
35	30	20	15	2.5	2.5	3

Table 2 Section properties of 40-story framed tube and reduced model (8-story)

No. of Stories	E (kN/m²)	I_c (m⁴)	I_b (m⁴)	A (m²)
40	2×10^7	0.03413	0.03413	0.64
8	2×10^7	0.853325	1.70665	0.64

Table 3 Displacements and rotations of frame tube 40-story and reduced model (8-story)

Program	Types of analysis	d_X (mm)	d_y (mm)	θ (rad)
SAP2000	Linear analysis	72.979	-29.697	0.000431
	Second-order analysis	73.860	-29.791	0.000437
MATLAB 40 Story	Linear analysis	78.368	-29.678	-0.000449
	Second-order analysis (Newton's Raphson)	79.396	-29.817	-0.000456
	Second-order analysis (Arc Length)	79.270	-29.771	-0.000456
MATLAB 8 Story (Reduced model)	Linear analysis	74.899	-31.720	-0.000455
	Second-order analysis (Newton's Raphson)	75.955	-31.868	-0.000463
	Second-order analysis (Arc Length)	75.956	-31.868	-0.000463

Table 4 Displacements and rotations of tube in tube 40-story and reduced model (8-story)

Program	Types of analysis	d_X (mm)	d_y (mm)	θ (rad)
SAP2000	Linear analysis	54.363	-21.15	0.000396
	Second-order analysis	54.840	-21.21	0.000400
MATLAB 40 Story	Linear analysis	57.628	-21.25	-0.000416
	Second-order analysis (Newton's Raphson)	58.173	-21.33	-0.000420
	Second-order analysis (Arc Length)	58.033	-21.28	-0.000419
MATLAB 8 Story (Reduced model)	Linear analysis	49.371	-22.47	-0.000399
	Second-order analysis (Newton's Raphson)	49.821	-22.54	-0.000403
	Second-order analysis (Arc Length)	49.822	-22.55	-0.000403

Table 5 Critical buckling load for 40-story buildings and reduced models

Frame tube (40-story)		Tube in tube (40-story)	
Program	**Critical buckling load (kN)**	**Program**	**Critical buckling load (kN)**
SAP2000	152654	SAP2000	199949
MATLAB 40-Story	144478	MATLAB 40-Story	191375
MATLAB 8-Story (Reduced model)	148091	MATLAB 8-Story (Reduced model)	213910

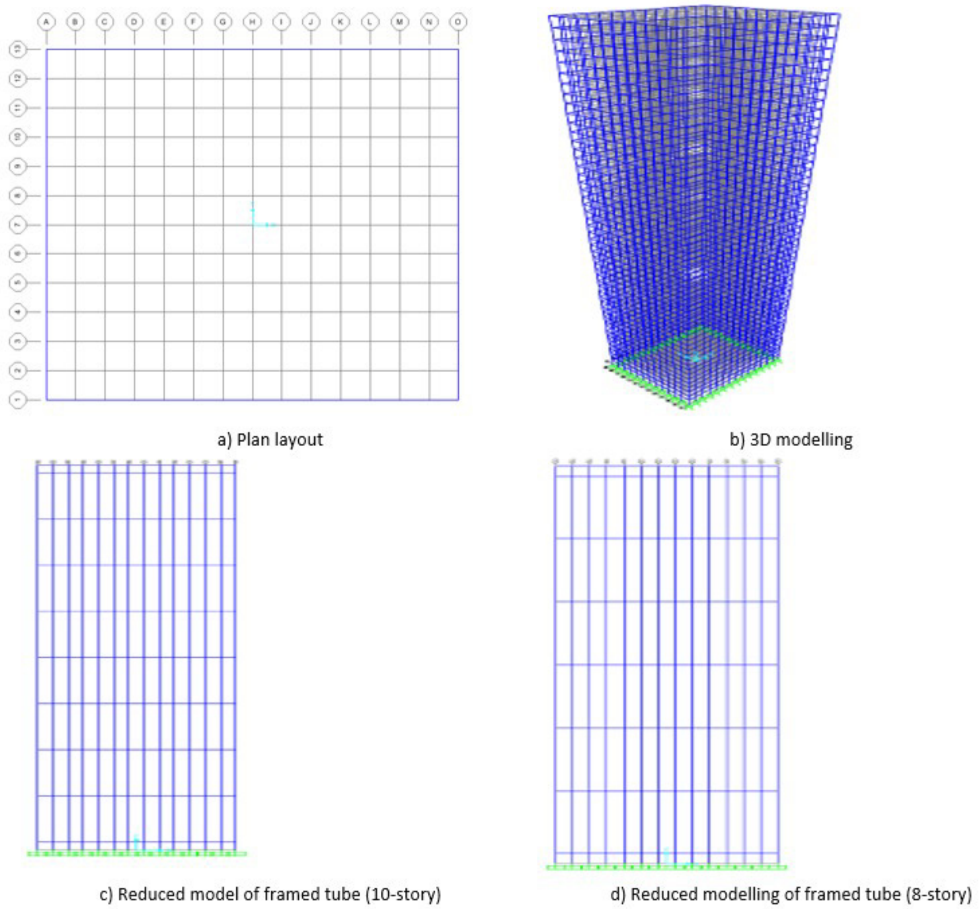

Figure 6 Plan layout, elevation view and 3D modelling of 40-story structure

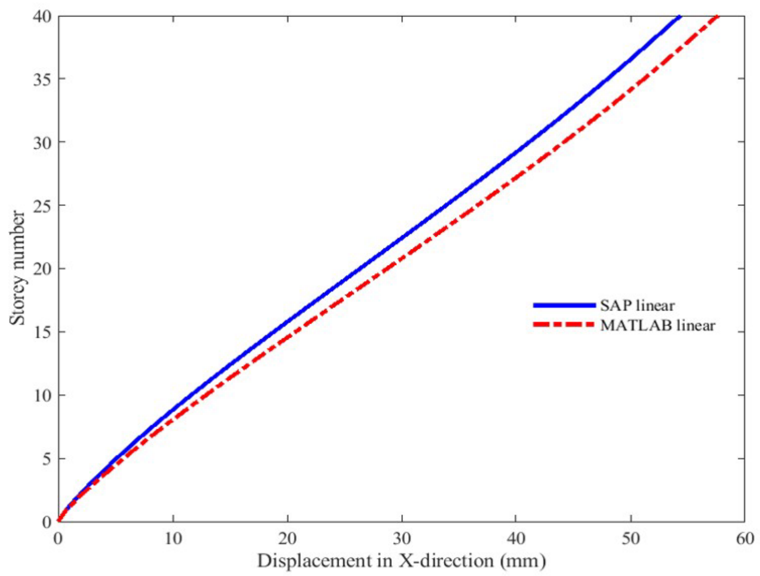

Figure 7 Diagram of the displacement in X-direction vs story number

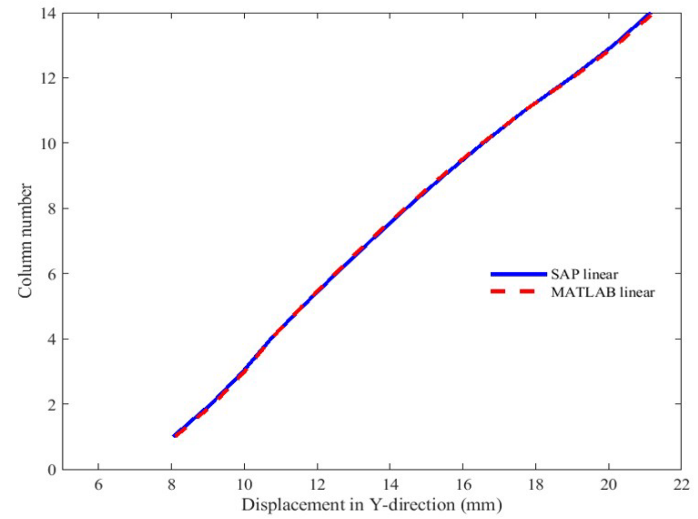

Figure 8 Diagram of the displacement in Y-direction vs column number

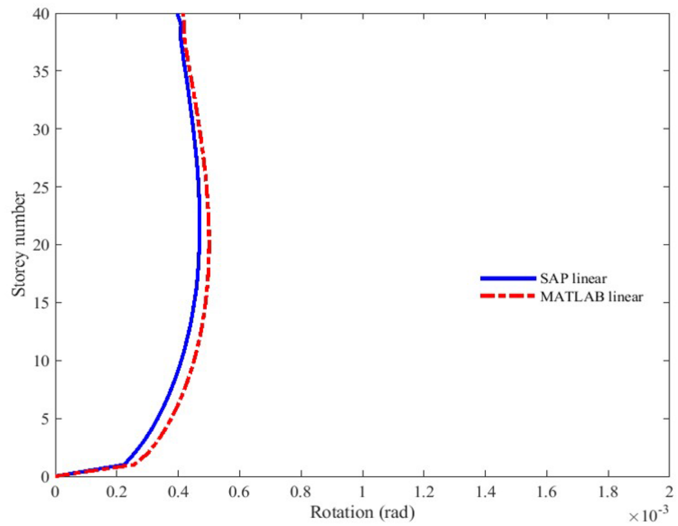

Figure 9 Diagram of the rotation vs story number

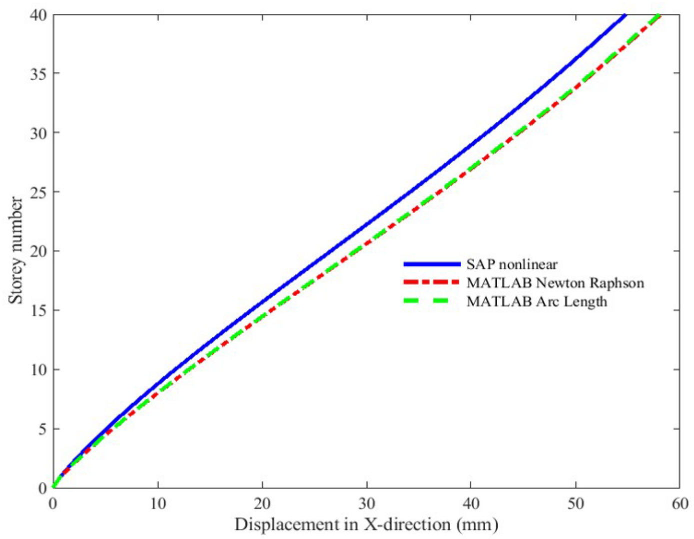

Figure 10 Diagram of the displacement in X-direction vs story number

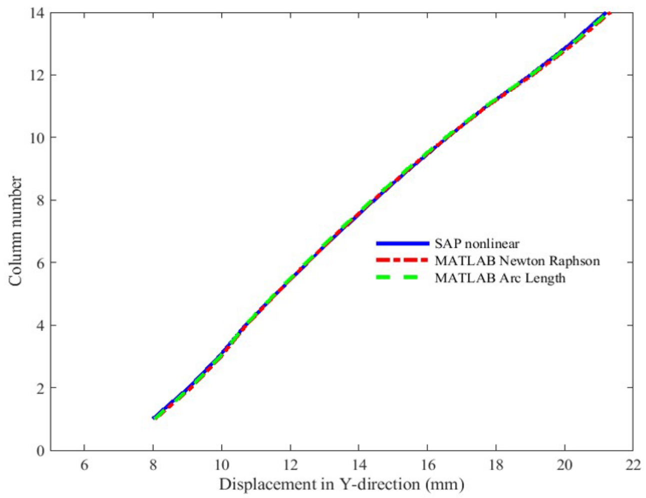

Figure 11 Diagram of the displacement in Y-direction vs column number

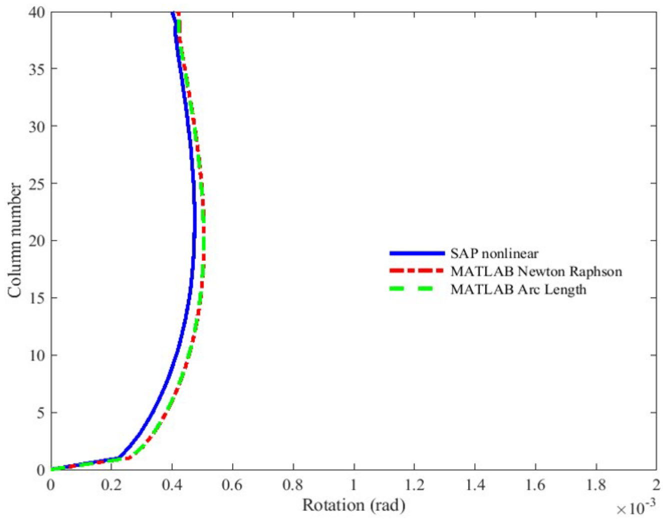

Figure 12 Diagram of the rotation vs story number

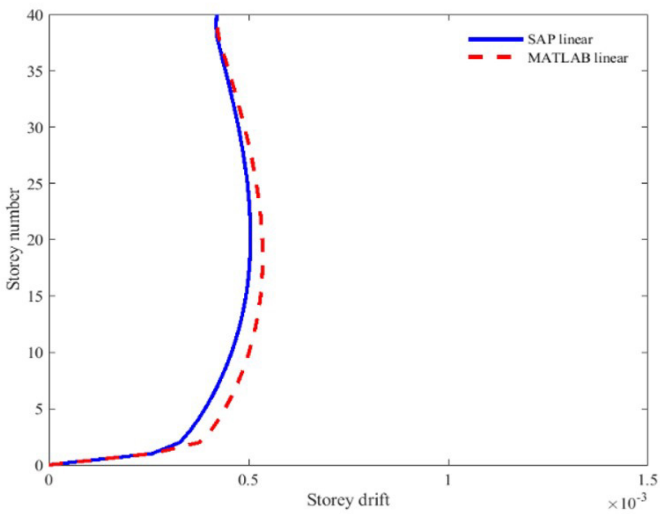

Figure 13 Diagram of the drift vs story number

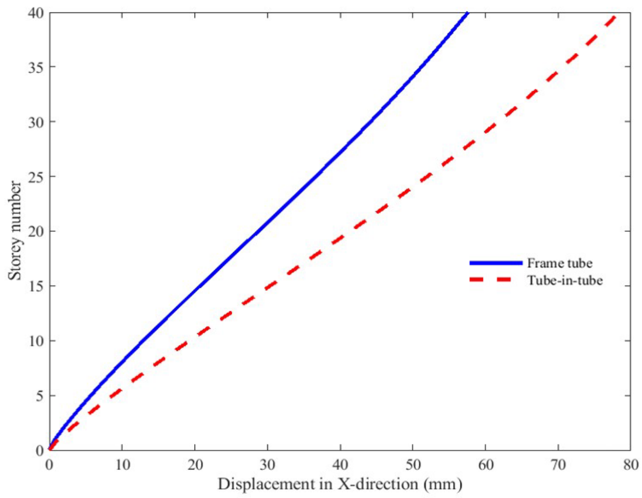

Figure 14 Comparison diagram of the displacement in X-direction vs story number

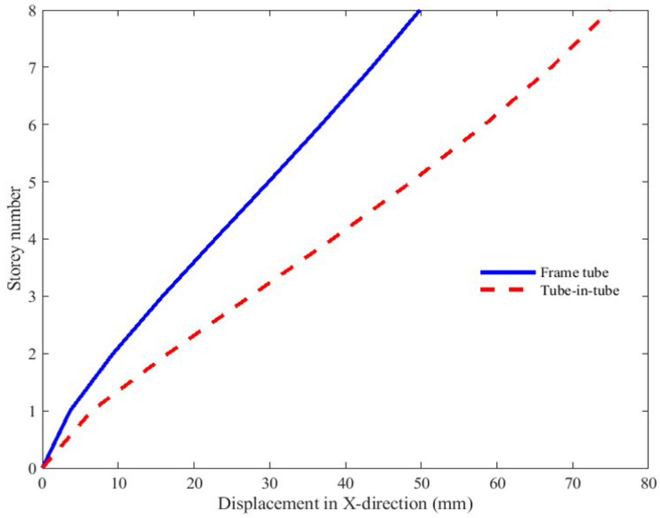

Figure 15 Reduced model comparison diagram of the displacement in X-direction vs story number

3.2 Example 2:

In the second example, two high-rise 50-story concrete models has been used. The first is the framed-tube structure with the reduced model and the second is the tube-in-tube structure with the reduced model. The dimensions of beams and columns are 0.8 meters by 0.8 meters. Floors are modeled with a height of 3.0 meters and columns with a distance of 2.5 meters. The modulus of elasticity is considered to be 20 GPa. Lateral and vertical loads are applied with a uniform distribution of 120 kN/m and 200 kN/m, respectively on the structures. Specifications of the structure are listed in Tables 6 and 7. Plan layout, elevation view, and 3D modeling of this example have been shown in Fig. 16. Also, displacements and rotations of tubular structures are shown in Tables 8-10 and Figs. 17-24.

Table 6 Dimensions of 50-story buildings

External frame tube dimensions		Internal frame tube dimensions		Distance from center to center of the columns		Story height
$2(W_f)_o$ (m)	$2(W_w)_o$ (m)	$2(W_f)_i$ (m)	$2(W_w)_i$ (m)	S_f (m)	S_w (m)	h (m)
50	30	20	10	2.5	2.5	3

Table 7 Section properties of 50-story framed tube and reduced model (10-story)

No. of Stories	E (kN/m^2)	I_c (m^4)	I_b (m^4)	A (m^2)
50	2×10^7	0.03413	0.03413	0.64
10	2×10^7	0.853325	1.70665	0.64

Table 8 Displacements and rotations of frame tube 50-story and reduced model (10-story)

Program	Types of analysis	d_x (mm)	d_y (mm)	θ (rad)
SAP2000	Linear analysis	151.925	-49.420	0.000884
	Second-order analysis	154.895	-49.725	0.000903
MATLAB 50-Story	Linear analysis	160.482	-49.402	-0.000902
	Second-order analysis (Newton's Raphson)	163.883	-49.842	-0.000923
	Second-order analysis (Arc Length)	163.368	-49.687	-0.000920
MATLAB 10-Story (Reduction model)	Linear analysis	155.456	-51.911	-0.000903
	Second-order analysis (Newton's Raphson)	158.988	-52.376	-0.000927
	Second-order analysis (Arc Length)	158.841	-52.328	-0.000926

Table 9 Displacements and rotations of tube-in-tube 50-story and reduced model (10-story)

Program	Types of analysis	d_x (mm)	d_y (mm)	θ (rad)
SAP2000	Linear Analysis	116.680	-35.235	0.000778
	Second-order analysis	118.411	-35.432	0.000791
MATLAB 50-Story	Linear analysis	121.844	-35.337	-0.000798
	Second-order analysis (Newton's Raphson)	123.775	-35.608	-0.000812
	Second-order analysis (Arc Length)	123.387	-35.497	-0.000809
MATLAB 10-Story (Reduced model)	Linear analysis	108.595	-36.811	-0.000775
	Second-order analysis (Newton's Raphson)	110.294	-37.069	-0.000788
	Second-order analysis (Arc Length)	110.224	-37.045	-0.000788

Table 10 Critical buckling load for 50 story buildings and reduced models

Frame tube 50-story		Tube in tube 50-story	
Program	Critical buckling load (kN)	Program	Critical buckling load (kN)
SAP2000	110294.8	SAP2000	140325
MATLAB 50-Story	105921.5	MATLAB 50-Story	136019
MATLAB 10-Story (Reduced model)	108050.3	MATLAB 10-Story (Reduced model)	147777

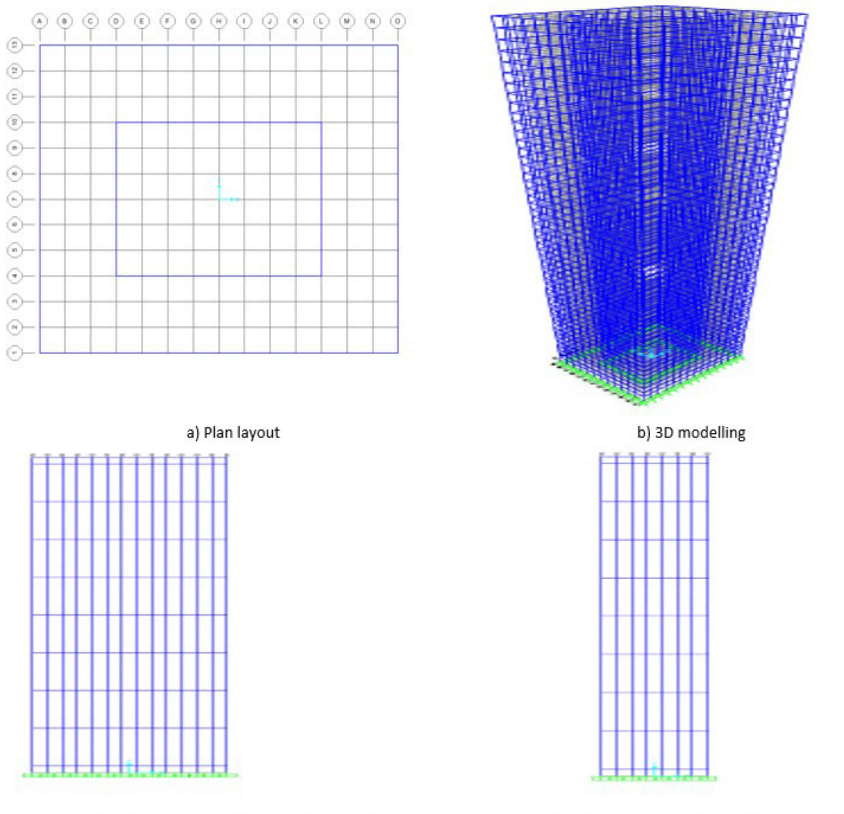

Figure 16 Plan layout, elevation view and 3D modelling of 50-story tube in tube structure

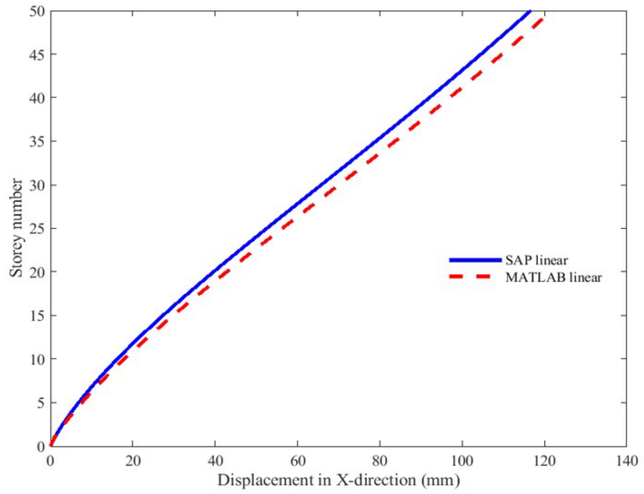

Figure 17 Diagram of the displacement in X-direction vs story number

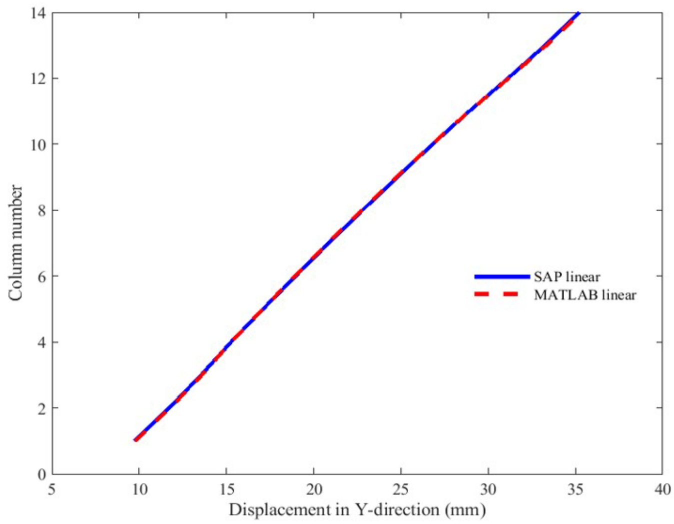

Figure 18 Diagram of the displacement in Y-direction vs column number

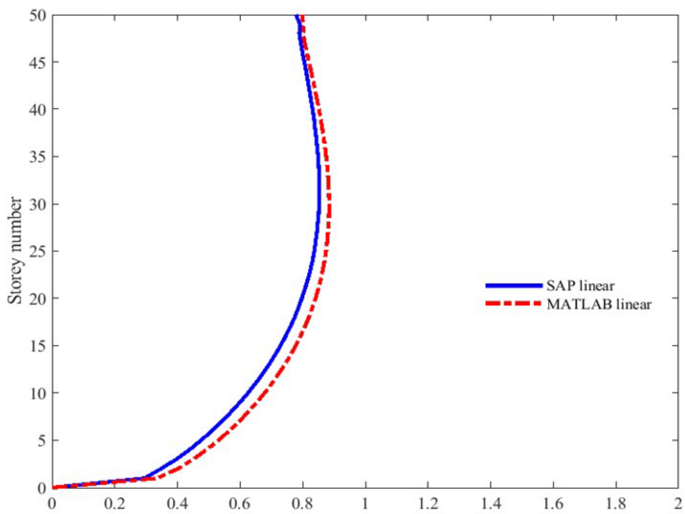

Figure 19 Diagram of the rotation vs story number

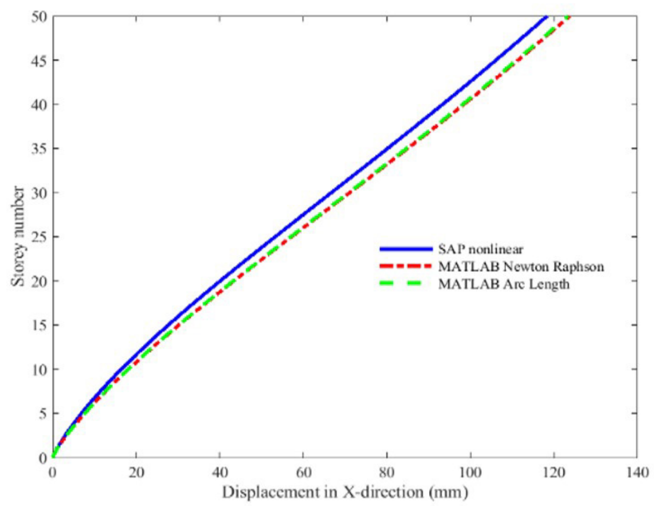

Figure 20 Diagram of the displacement in X-direction vs story number

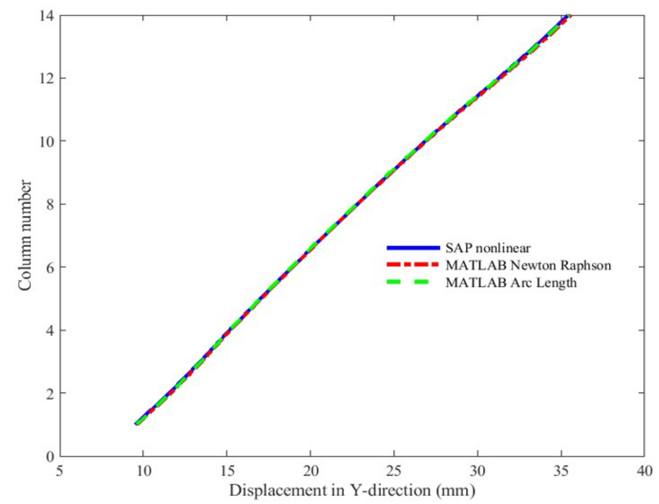

Figure 21 Diagram of the displacement in Y-direction vs column number

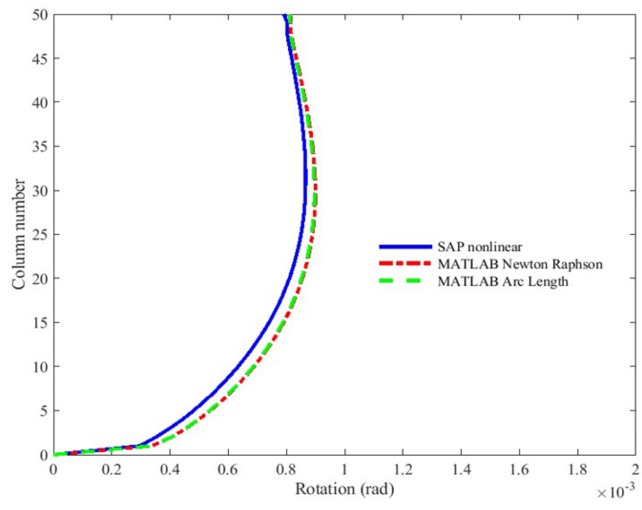

Figure 22 Diagram of the rotation vs story number

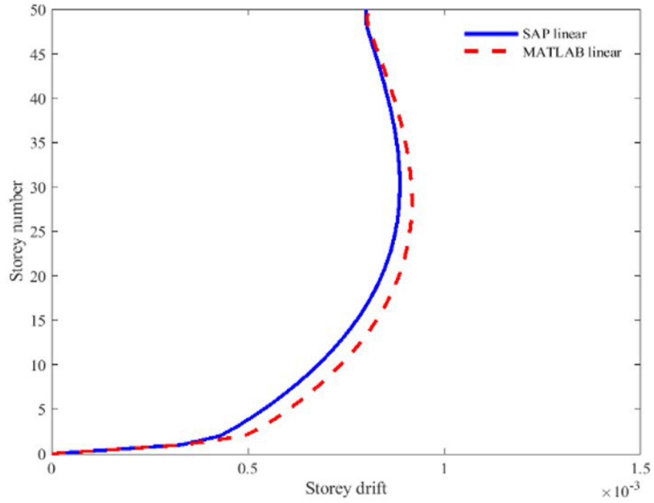

Figure 23 Diagram of the drift vs story number

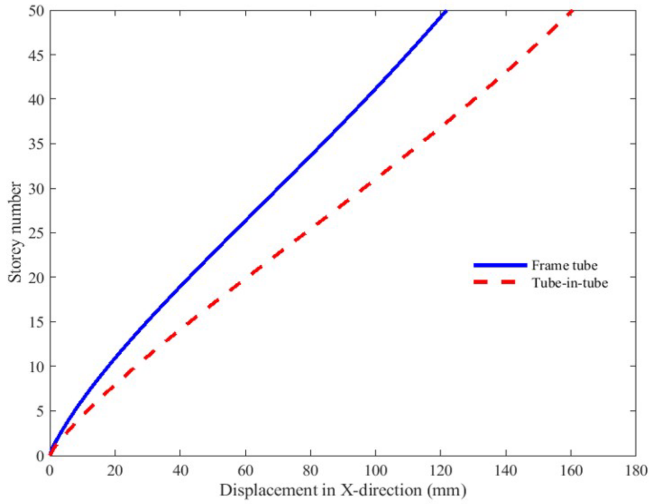

Figure 24 Comparison diagram of the displacement in X-direction vs story number

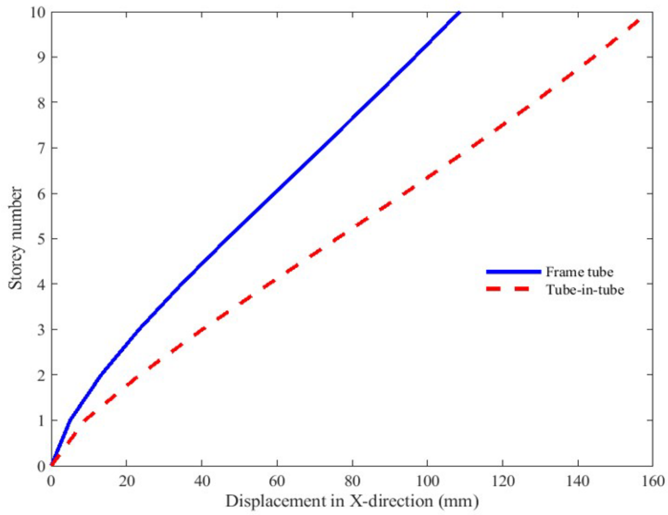

Figure 25 Reduced model comparison diagram of the displacement in X-direction vs story number

4 RESULTS

In this research, tall buildings 40 and 50 stories have been used for modeling. For each structure, two framed-tube and tube-in-tube systems are considered. All structures are modeled in three-dimensional in SAP2000 software. Also, the desired structures are coded in MATLAB software in two-dimensional and reduced form. After running the programs in MATLAB and SAP2000 software, the responses of the structures have been presented in the form of tables and figures.

The results of the analysis of 40-story structures are shown in Tables 3-5 and Figs. 7-15. Also, the results of the analysis of 50-story structures are shown in Tables 8-10 and Figs. 16-24. The number of beams and nodes for building models of 40 and 50 stories are shown in Tables 11 and 12, respectively. As it is clear from the tables and figures, displacements in structures with framed-tube systems have been reduced by about 30% using structures with tube-in-tube systems. This reduction in displacement is due to the addition of an internal frame and increasing the stiffness of the tube-in-tube system compared to the framed-tube system.

In the nonlinear analysis, due to the reduction of the stiffness matrix of the structure by the geometric matrix, the displacements and rotations have been increased by 6% compared to the linear mode. Nonlinear analysis has been done using two methods, Newton's Raphson and Arch Length, and the slight difference in the results of the two methods shows that the modeling is done correctly. The results reported in the tables show that in the tube-in-tube system, the critical load has been increased by about 27% compared to the framed tube system due to the increase in stiffness. Also, the critical load in 50-story structures has been decreased by about 25% compared to 40-story structures.

The displacement of the framed tube and tube-in-tube systems for the 40-story models and its reduced to 8-story are shown in Figs. 13 and 14. Also, the displacement of the framed-tube and tube-in-tube systems for the 50-story model and its reduced to 10-story are shown in Figs. 24 and 25.

It can be seen, that the displacement of the reduced models is about 5% different from the original models. As a result, the proposed method can provide acceptable results with less time and acceptable accuracy. The proposed method can be used instead of the three-dimensional analysis of the actual model with a much smaller number of nodes and elements and a significant reduction in calculations and analysis time. The number of beam elements and nodes of 3D, 2D, and proposed models are listed in the tables. According to the results of Table 13, it can be seen that the proposed method has reduced the volume of calculations by 80% along with a 5% decrease in the accuracy of structural responses.

Table 11 Number of beams and nodes for 40-story building models

Models	40-story (3D)		40-story (2D)		40-story (Reduced model)	
	Number of Elements	Number of nodes	Number of Elements	Number of nodes	Number of Elements	Number of nodes
Framed-tube	4160	2132	1080	574	216	126
Tube-in-tube	6400	3280	1640	861	336	198

Table 12 Number of beams and nodes for 50-story building models

Models	50 story (3D)		50 story (2D)		50 story (Reduced model)	
	Number of Elements	Number of nodes	Number of Elements	Number of nodes	Number of Elements	Number of nodes
Framed-tube	5200	2652	1350	714	270	154
Tube-in-tube	8000	4080	2050	1071	420	242

Table 13 Accuracy and volume of calculations of the reduced models

Models		Reduced element (%)	Reduced node (%)	Decrease accuracy (%)
40 story	**Framed-tube**	80	78	5
	Tube-in-tube	80	77	5
50 story	**Framed-tube**	80	78	5
	Tube-in-tube	80	77	5

5 CONCLUSION

In this research, has been proposed an innovative method to convert the modeling of three-dimensional structures to the modeling of two-dimensional structures for the stability analysis of long tubular buildings. The accuracy and speed of analysis of the new method have been checked by comparing the displacements and drifts in the modeled. The proposed method could be applied for tubular tall structures with symmetric plans and regular height with any stories. Nonlinear equations were solved by Newton's Raphson method and Arc Length, and the answers were obtained with a very small difference of 3-5%. The process of the proposed method is in the form of modeling the equivalent frame and then modeling the reduced frame using the equivalent moment of inertia for beams and columns. The drift calculated based on the proposed and reduced model was obtained similar to the values of the actual models with acceptable accuracy. Converting the three-dimensional structure into a two-dimensional structure and the reduced model, a very large number of elements and nodes of the original structure were reduced. Finally, with very few calculations in a short time and with a small error, the desired analysis was done and the corresponding answers were obtained. It was shown that the proposed method has reduced the amount of calculations by 80% along with a 5% reduction in the accuracy of structural responses.

Author's Contribuitions: Methodology, Validation, Formal analysis, Investigation, Writing original draft, Javad Firouzbakhsh; Conceptualization, Reviewing and editing, Supervision, Project administration, Reza Rahgozar and Mohsen Malekinejad.

Editor: Pablo Andrés Muñoz Rojas

References

Ali, M. M. and Al-Kodmany, K. (2022). Structural systems for tall buildings. Encyclopedia, 2(3), 1260-1286.

Aydin S. and Bozdogan K. B. (2016). Lateral stability analysis of multistory buildings using the differential transform method. Structural Engineering and Mechanics. 57(5), 861-876.

Bozdogan, K. B. and Ozturk, D. (2014). Free vibration analysis of the tube-in-tube tall buildings with the differential transform method. Advances in Structural Engineering, 17(9), 1271-1279.

Chan, S. L. and Chui, P. T. (Eds.). (2000). Non-linear static and cyclic analysis of steel frames with semi-rigid connections. Elsevier.

Dadkhah, M., Kamgar, R. and Heidarzadeh, H. (2022). Reducing the cost of calculations for incremental dynamic analysis of building structures using the discrete wavelet transform. Journal of Earthquake Engineering, 26(7), 3317-3342.

Davari, S. M., Rahgozar, R. and Malekinejad, M. (2019). A simple method for static analysis of tubular high-rise buildings using Timoshenko beam theory. Intenational Journal of Engineering and Technology, 11(3), 563-575.

Dua, R. and Jain, A. K. (2004). Seismic bifurcation for response-control of tall building structures. International Journal of Structural Stability and Dynamics, 4(2), 197-221.

Gunel, M. H. and Ilgin, H. E. (2007). A proposal for the classification of structural systems of tall buildings. Building and Environment, 42(7), 2667-2675.

Hariri-Ardebili, M. A., Rahmani-Samani, H. and Mirtaheri, M. (2014). Seismic stability assessment of a high-rise concrete tower utilizing endurance time analysis. International Journal of Structural Stability and Dynamics, 14(6), 1450016.

Hosseini, O., Malekinejad, M. and Rahgozar, R. (2012). A closed form solution for free vibration analysis of tube-in-tube systems in tall buildings. International Journal of Engineering, 25(2), 107-114.

Jahanshahi, M. R., Malekinejad, M. and Rahgozar, R. (2012). A simple approach to static analysis of tall buildings with a combined tube-in-tube and outrigger-belt truss system subjected to lateral loading. International Journal of Engineering, 25(3), 289-300.

Kwan, A. K. (1994). Simple method for approximate analysis of framed tube structures. Journal of Structural Engineering, 120(4), 1221-1239.

Lavanya, T. S. and Sridhar, S. (2017). Dynamic analysis of tube-in-tube tall buildings. International ResearchJjournal of Engineering and Technology, 4(4), 2357-2362.

Li, G. Q., Ding, X. and and Chen, S. W. (2010). On inter-storey drift limitation of steel–concrete hybrid structures for tall buildings. Journal of Earthquake and Tsunami, 4(1), 1-7.

Li, Y., Li, C., Li, Q. S., Li, Y. G. and Chen, F. B. (2021). Refined mathematical models for across-wind loads of rectangular tall buildings with aerodynamic modifications. International Journal of Structural Stability and Dynamics, 21(9), 2150131.

Li, Z., Huang, G., Chen, X. and Zhou, X. (2022). Seismic response and parametric analysis of inter-story isolated tall buildings based on enhanced simplified dynamic model. International Journal of Structural Stability and Dynamics, 22(3-4), 2240008.

Malekinejad, M. and Rahgozar, R. (2011). Free vibration analysis of tall buildings with outrigger-belt truss system. Earthquake and Structures, 2(1), 89-107.

Malekinejad, M. and Rahgozar, R. (2012). A simple analytic method for computing the natural frequencies and mode shapes of tall buildings. Applied Mathematical Modelling, 36(8), 3419-3432.

McGuire, W., Gallagher, R. H. and Ziemian, R. D. (2000). Matrix Structural Analysis. 2nd Edition, John Wiley & Sons.

Naik, B. H. and Chandra, B. S. (2017). Comparative analysis between tube in tube structure and conventional moment resisting frame. International Research Journal of Engineering and Technology, 4(10), 808-812.

Parv, B. R. and Nicoreac, M. P. (2012). Global structural analysis of central cores supported tall buildings compared with FEM. Acta Tecnica Napocensis: Civil Engineering & Architecture, 55(3), 251-262.

Prinz, G. S. and Richards, P. W. (2024). Experimental evaluation and design procedure for all-steel tube-in-tube buckling restrained braces. Journal of Structural Engineering, 150(1): 04023201, doi: 10.1061/jsendh.steng-12566.

Rahgozar, P. (2020). Free vibration of tall buildings using energy method and Hamilton's principle. Civil Engineering Journal, 6(5), 945-953.

Rahgozar, R. and Sharifi, Y. (2009). An approximate analysis of combined system of framed tube, shear core and belt truss in high-rise buildings. The Structural Design of Tall and Special Buildings, 18(6), 607-624.

Rahgozar, R., Ahmadi, A. R. and Sharifi, Y. (2010). A simple mathematical model for approximate analysis of tall buildings. Applied Mathematical Modelling, 34(9), 2437-2451.

Rahgozar, R., Mahmoudzadeh, Z., Malekinejad, M. and Rahgozar, P. (2015). Dynamic analysis of combined system of framed tube and shear walls by Galerkin method using B-spline functions. The Structural Design of Tall and Special Buildings, 24(8), 591-606.

Sharma, A. and Gurjar, C. (2024). Seismic analysis of RCC tube-in-tube structure with different shape of building with constant cross sectional area:-A Review, International Research Journal of Modernization in Engineering Technology and Science, 6, doi: 10.56726/IRJMETS48126.

Smith, J. and Coull, A. (1991). Tall Building Structures, Analysis & Design. Wiley and Sons, New York.

Takabatake, H. (2010). Two-dimensional rod theory for approximate analysis of building structures. Earthquakes and Structures, 1(1), 1.

Taranath, B. S. (2016). Structural analysis and design of tall buildings: Steel and composite construction. CRC Press.

Tehranizadeh, M., Shamlu, M. and Taslimi, A. (2019). A simplified method to conform 3D symmetric RC core walls to equivalent planar systems. In Proceeding of the 11th National Congress on Civil Engineering, Shiraz University, Shiraz, Iran.

Zalka, K. A. (1979). Buckling of a cantilever subjected to distributed normal loads, taking shearing deformation into account. Acta Technica Hung. 89(3-4), 497-508.

Zalka, K. A. (2002). Buckling analysis of buildings braced by frameworks, shear walls and cores. The Structural Design of Tall and Special Buildings. 11(3), 197-219.</jrn>

Appendix A

Step-by-step Newton-Raphson algorithm for geometric nonlinear analysis:

Definition of variables and parameters.

The first load increment {ΔF}, enter the boundary conditions, the relationship between the elements, the geometry of the structure, the characteristics of the materials and the maximum number of increments.

Form the tangential stiffness matrix of each member [kt].

Transfer the stiffness matrix from the local coordinate to the global coordinate using the transfer matrix [T].

Form the global stiffness matrix of the structure by assembling the stiffness matrix of the members [Kt].

Incremental displacement calculation using:

$$\{\Delta U\} = [k_t]^{-1}\{\Delta F\} \tag{A.1}$$

Updating the geometry of the structure based on the last displacement:

$$\{U\} = \{U\} + \{\Delta U\} \tag{A.2}$$

Calculation of internal force vector of members in global coordinates {Pint}.

Calculation of the unbalanced force vector using the relation:

$$\{Q\} = \{F_{ext}\} - \{P_{\text{int}}\} \tag{A.3}$$

Calculation {Δu} using equation:

$$\{K_t\}\{F_{ext}\} = \{Q\} \tag{A.4}$$

If the convergence criterion is not satisfied, the new geometry of the structure is updated using relation $\{U\} = \{U\} + \{\Delta U\}$, and steps 8 to 11 are repeated until reaching the desired convergence.

The convergence criterion can be written as follows based on displacement control:

$$\sqrt{\frac{\left\|\{\Delta u\}\right\|}{\left\|\{u\}\right\|}} = \left(\frac{\sum_{i=1}^{DOF}\left(\Delta u_i\right)^2}{\sum_{i=1}^{DOF}\left(u_i\right)^2}\right)^{0.5} \le \varepsilon; \qquad \varepsilon \simeq 1\times10^{-3} \tag{A.5}$$

Apply the new load increment {ΔF} and return to step 1. When the number of increments reaches the value specified in the input, the calculations will end.

Appendix B

Step-by-step Arc Length of cylinders algorithm for geometric nonlinear analysis:

Definition of variables and parameters, considering the external load vector Fext, Specifying the maximum number of increments.

Predict or increment phase

Start from the convergence point at the end of the previous step $(u_{\circ}, \lambda_{\circ} F_{ext})$.

Values $\Delta\lambda_1$ and Δu_1 are obtained using the following equation at the beginning of the predict phase or increment:

$$\delta u_t = K_t^{-1} F_{ext} \Rightarrow \Delta\lambda_1 = \pm \frac{\Delta L}{\sqrt{\delta u_t^{\,T} \delta u_t}} \tag{B.1}$$

Kt, the global stiffness matrix of the structure calculated at displacement $u_{\circ}$. The sign $\pm$ is the same sign as the determinant of the stiffness matrix.

$$\Delta u_t = \Delta\lambda_1 \delta u_t \tag{B.2}$$

Note: For the first increment in the first step $u_{\circ} = 0$, a suitable value for $\Delta\lambda_1$ or ΔL should be considered.

Having Δu_1 and $\Delta\lambda_1$, which are the same as Δu_0 and $\Delta\lambda_{\circ}$, the next point is $(u_1, \lambda_1 F_{ext})$. This point is also called $(u_P, \lambda_P F_{ext})$ because it is obtained from predict phase.

$$\begin{aligned} \Delta u_1 &= \delta u_0 \Rightarrow u_1 = u_0 + \Delta u_1 \\ \Delta\lambda_1 &= \delta\lambda_0 \Rightarrow \lambda_1 = \lambda_0 + \Delta\lambda_1 \end{aligned} \tag{B.3}$$

Calculation of internal force vector of members in global coordinates {Pint}, Considering the displacement calculated in the previous step (deformed geometry of the structure).

Calculation of the unbalanced force vector using the relation:

$$Q = \lambda F_{ext} - P_{\text{int}} \tag{B.4}$$

Correction or iteration phases

In this phase, the values $\Delta u_{old}, \Delta\lambda_{old}$ and Q old are input.

The following displacement vectors are calculated:

$$\begin{aligned} \delta u_t &= K_t^{-1} F_{ext} \\ \delta\overline{u} &= K_t^{-1} Q_{old} \end{aligned} \tag{B.5}$$

Calculation of scalar coefficients from a1 to a5:

$$\begin{aligned} a_1 &= \delta u_t^{\,T} \delta U_t \\ a_2 &= 2\delta u_t \left(\Delta u_{old} + \delta\overline{u}\right) \\ a_3 &= \left(\Delta u_{old} + \delta\overline{u}\right)^T \left(\Delta u_{old} + \delta\overline{u}\right) - \Delta L^2 \\ a_4 &= \frac{\Delta u_{old}^{\,T} \left(\Delta u_{old} + \delta\overline{u}\right)}{\Delta L^2} \\ a_5 &= \frac{\Delta u_{old}^{\,T} \delta\overline{u}}{\Delta L^2} \end{aligned} \tag{B.6}$$

Solving quadratic equation $a_1\delta\lambda^2 + a_2\delta\lambda + a_3 = 0$ to calculate $\delta\lambda$.

If the equation has two real roots $\Delta\lambda_1$ and $\Delta\lambda_2$:

Also, if it is $(a_4 + a_5\delta\lambda_1) > (a_4 + a_5\delta\lambda_2)$, the answer to the equation is $\Delta\lambda_1$. Otherwise, the answer is $\delta\lambda_2$.

If it is $a_1 = 0$, the answer to the equation is $\delta\lambda = -a_3/a_2$.

If the answers to the equation are imaginary, ΔL should be halved and repeat the calculations from step 7 with this new arc length.

Updating load factor (λ) and calculating load factor $(\Delta\lambda)$ for the next iteration:

$$\lambda_{new} = \lambda_{old} + \delta\lambda$$
$$\Delta\lambda_{new} = \Delta\lambda_{old} + \delta\lambda \tag{B.7}$$

Updating displacement vector (u) and calculating displacement increment (Δu) for the next iteration:

$$\delta u_{new} = \delta\overline{u} + \delta\lambda\delta u_t$$
$$\Delta u_{new} = \Delta u_{old} + \delta u_{new} \Rightarrow u_{new} = u_\circ + \Delta u_{new} \tag{B.8}$$

In this step, the new point $(u_{new}, \lambda_{new}F_{ext})$ is obtained.

Calculation of internal force vector of members in global coordinates {Pint},Based on the latest geometry of the structure.

Calculation of the unbalanced force vector using the relation:

$$Q = \lambda F_{ext} - P_{\text{int}} \tag{B.9}$$

Convergence control: If the convergence criterion is not satisfied, with the last $\Delta u, \Delta\lambda_1$ and Q now taking the index old, we repeat steps 7 to 13 until reaching the desired convergence.

The convergence criterion can be written as follows based on displacement control:

$$\sqrt{\frac{\|\delta u_{new}\|}{\|u_{new}\|}} = \left(\frac{\sum_{i=1}^{DOF}(\delta u_i)^2}{\sum_{i=1}^{DOF}(u_i)^2}\right)^{0.5} \leq \varepsilon; \qquad \varepsilon \simeq 1\times10^{-3} \tag{B.10}$$

Determining the length of the arc for the next increment based on the following relationship:

$$\Delta L_{new} = \Delta L_{old}\left(\frac{I_{des}}{I_{old}}\right)^{0.5}; \qquad I_{des} \simeq 3 \tag{B.11}$$

Return to step 2 and start from the new convergence point $(u_{new}, \lambda_{new}F_{ext})$, which now takes index o. When the number of increments reaches the value specified in the input, the calculations will end.